Neurostimulation Strategy for Stress Urinary Incontinence

Xuechen Huang, Kaihui Zheng, Sam Kohan, Petcharat May Denprasert, Limin Liao, and Gerald Eli Loeb, *Senior Member, IEEE*

***Abstract*— We have developed a percutaneously implantable and wireless microstimulator (NuStim) to exercise the pelvic floor muscles for the treatment of stress urinary incontinence. It produces a wide range of charge-regulated electrical stimulation pulses and trains of pulses using a simple electronic circuit that receives power and timing information from an externally generated RF magnetic field. The complete system was validated *in vitro* and *in vivo* in preclinical studies demonstrating that the NuStim can be successfully implanted into an effective, low threshold location, and the implant can be operated chronically to produce effective and well-tolerated contractions of skeletal muscle.**

***Index Terms*— Neuromuscular stimulation, implant, wireless.**

I. Introduction

STRESS urinary incontinence (SUI) is a common type of incontinence with symptoms of involuntary leakage of urine during activities that increase intra-abdominal pressure (e.g., coughing, sneezing or laughing). The majority of patients with mild to moderate SUI have weakness of the external urethral sphincter (EUS) and pelvic floor muscle, usually as a result of damage during childbirth or surgery and often exacerbated by hypotrophic changes associated with aging and declining hormone levels [1]. Chronic urinary incontinence is a common condition associated with severe medical and social consequences [2].

Like any striated skeletal muscle, the EUS with intact neuromuscular innervation responds to exercise by increasing its bulk and strength. This is the basis of pelvic floor muscle training (PFMT, also known as Kegel exercise), which is highly effective when done properly and conscientiously [3]. Significant improvement of muscle function requires proper instruction and regular and persistent exercise for at least several months. If PMFT is initially successful, the benefits appear to persist [4]. However, PFMT is difficult to perform correctly, and few patients are trained properly or sufficiently disciplined to perform the exercise often and long enough to obtain substantial benefit. Thus, patients with SUI are often subjected to surgical procedures or pharmacological treatments rather than PMFT.

Pharmacological therapy achieves varying degrees of success, but with substantial side effects [5]. Surgery is recommended for many patients who fail to respond to an initial trial of PMFT. While the surgical treatment causes minimal to moderate pain and discomfort, it is an invasive surgical procedure with general risk of complications from anesthesia and wound infections. There are also specific complications such as inadvertent mechanical damage to the bladder or urethra (perforation), or difficulty in urinating after surgery [6] {Novara, 2008 #60;Petri, 2012 #119}. The most commonly used surgical procedure is the tension-free vaginal tape (TVT) suspension. TVT has an initially high success rate (75-95%), but incontinence may recur over time and requires repeat surgery with significantly more adverse events and less success than the initial procedure [5]. Recently, some tape products have been voluntarily recalled after increased reports of severe long-term complications, including erosion and perforation of tissues such as the vaginal wall [7].

Rather than relying on voluntary PFMT, it may be possible to achieve the same trophic effects on muscle fibers by activating them by neuromuscular electrical stimulation (NMES) [8], [9]. Because the muscle nerves lie under highly innervated skin and mucosa, commercial stimulators that use transcutaneous, intravaginal, or intrarectal electrodes are often unacceptable to patients due to somatosensory nerve excitation with unpleasant sensations [9], [10]. Transcutaneous magnetic stimulation (similar to transcranial magnetic stimulation, TMS) can induce eddy currents in the pelvis that are capable of activating muscle nerves, but this requires high-power, expensive instrumentation in a clinic [10]. Intramuscular electrodes can excite the terminal branches of motor axons with little or no sensation other than from the muscle contraction itself. Conventional implantable stimulators first used by Caldwell achieved efficacy for SUI without adherence problems, but the bulky case and long leads required invasive surgery with a risk of infection and high possibility of lead dislodgement [11].

Compared with previous NMES strategies, a fully implantable leadless stimulator could be a solution. We have developed a percutaneously implantable and wireless micros-

Manuscript received October 1, 2016; revised January 13, 2017; accepted February 26, 2017. Date of publication March 7, 2017; date of current version August 6, 2017. This work was supported by the General Stim Inc.

X. Huang and G. E. Loeb are with the Medical Device Development Facility, Department of Biomedical Engineering, University of Southern California, Los Angeles, CA 90089 USA, and also with General Stim Inc., Los Angeles, CA 90007 USA (e-mail: xuechenh@usc.edu; gloeb@usc.edu).

K. Zheng was with General Stim Inc., Los Angeles, CA 90007 USA. He is now with St. Jude Medical, Saint Paul, MN, USA.

S. Kohan and P. M. Denprasert are with General Stim Inc., Los Angeles, CA 90007 USA.

L. Liao is with the Department of Urology, China Rehabilitation Research Center, Beijing 100071, China, and also with the Rehabilitation School, Capital Medical University, Beijing 100069, China (e-mail: lmliao@263.net).

Digital Object Identifier 10.1109/TNSRE.2017.2679077

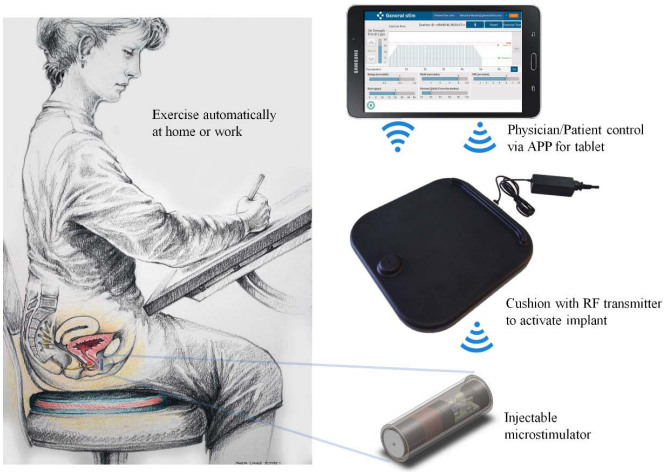

Fig. 1. Concept of NuStim operation. The patient receives passive exercise while sitting on the RF-Cushion and performing daily activities. Exercise is adjusted on a tablet and transmitted wirelessly to the RF-Cushion, which wirelessly powers and controls the implanted microstimulator.

timulator (NuStim®) that can be implanted into the pelvic floor muscles to generate strong contractions without producing unpleasant sensations or requiring voluntary effort. Although a similar fully implantable microstimulator (the BION®) was described 15 years ago [12], [13], it has not been commercially available, partly because it utilized fairly expensive technologies that were not cost-effective for applications like SUI that are problematic but not life-threatening. Compared to conventional surgical treatments for stress incontinence, we hypothesize that the NuStim treatment will be less invasive, less expensive, and have fewer post-operative and long-term complications, while achieving significant reduction of urinary leakage in patients with moderate stress incontinence from innervated but hypotrophic muscle. This paper describes the functional requirements, technological strategies, and *in vitro* and *in vivo* testing of this device.

II. Design

A. System Operation and Requirements

The NuStim has been designed as a low cost, minimally invasive, wireless system that patients can use at home to deliver precisely prescribed and reproducibly delivered NMES to a single site in the pelvic floor over a period of up to one year of PFMT for the treatment of SUI. The NuStim system contains three major subsystems (Fig. 1): an implanted microstimulator for chronic electrical stimulation, an external transmitter in a seat cushion, and a remote control in an Android smart-phone/tablet app.

The design requirements as listed below were derived from the therapeutic strategy:

- The microstimulator is small enough to be implanted accurately into the desired location via minimally invasive procedures.
- Control of various stimulus parameters is sufficient to achieve therapeutic effects for a range of electrode locations.
- Power and commands are transmitted wirelessly to the implant from outside the body.
- Packaging method can achieve required, limited longevity without expensive or bulky technologies.
- Using low-cost off-the-shelf components reduces both non-recurring engineering development and manufacturing costs.
- Graphical user interface enables easy clinical programming in professional setting and patient self-treatment at home.

B. Implant

1) Mechanical: The NuStim implant (3.4 mm diameter × 10 mm long) is designed for chronic implantation with projected functional life at least 1 year (Fig. 2a). It avoids expensive integrated circuits and hermetic packaging. The exterior consists of a borosilicate glass tube with a platinum/iridium (80%/20%) electrode on each end. The electronic circuitry consists of a two-sided ceramic printed circuit board (PCB; Fig. 2b), on which discrete electronic components are surface-mounted by reflow soldering (Fig. 2c). The externally generated RF magnetic field is received by a coil wound on a machined ferrite core (26.5 turns of 3-mil insulated copper; Fig. 2d) that serves as a substrate for the ceramic PCB (Fig. 2e). Wirebonds from the top of the large central component (programmable unijunction transistor – PUT; CP622-2N6027-CT, Central Semiconductor Corp, NY, USA) and connections to the electrodes are added to the ceramic PCB (Fig. 2f). The electronic subassembly slides into a glass tube (Fig. 2g), which is then attached to plastic tubes that apply vacuum to one side and inject centrifuged and de-gassed epoxy (Epotek #302-3M, Epoxy Technology Inc.) under pressure on the other side (Figs. 2h-i). After curing under pressure at 40C for 12h, the tubing and excess epoxy is removed from the ends, leaving the finished implant (Fig, 2j). With proper cleaning procedures before encapsulation, a strong adhesion between the epoxy and the surfaces of the electronic components prevents water condensation and corrosion [14].

2) Electronic: The circuitry relies on low-cost, off-the-shelf, surface mount components in a limited space to achieve functions of inductive power reception and pulse generation (schematic diagram and idealized waveforms in Fig. 3). We elected to control the charge per pulse rather than voltage or current because this is the determinant of stimulus strength for short pulses in which most of the charge is delivered faster than the 150 μs time constant of the myelinated motor axons.

The inductive coupling between the primary coil in the RF-Cushion and the secondary coil in the implant is very weak, and thus required systematic analysis to maximize the magnetic field capture by the small-sized implant, as discussed by Vest *et al.* [15]. The ferrite in the implant enhances the capture of magnetic flux, particularly if the axis of the implant is tilted with respect to the applied magnetic field. The inductive coil L2 and tuning capacitor C2 in parallel resonate at the carrier frequency to maximize the amplitude of the received RF signal, which is then half-wave rectified by

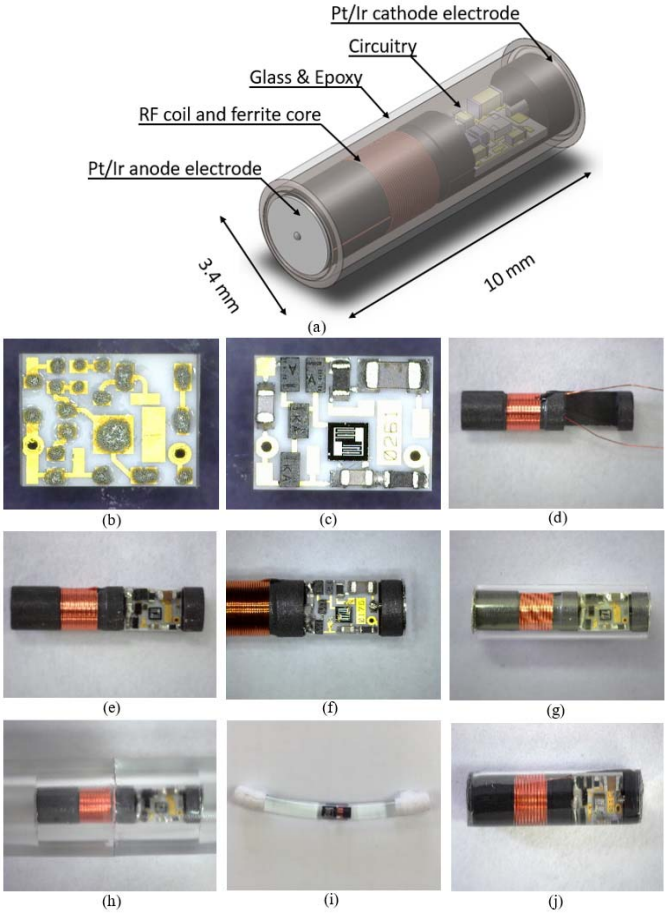

Fig. 2. *a*. Design of NuStim implant. *b-j*. Construction steps. *b*. Lead free solder paste is applied on the PCB. *c*. The surface-mount components are placed and soldered on hot plate (240°C for 30s). *d*. Ferrite is wound with insulated copper wire and cleaned in ultrasound. *e*. PCB is mounted on the ferrite with epoxy. *f*. coil terminals and electrodes are soldered. Wirebonds are placed to connect the PUT. *g*. Device is inserted and tacked inside the glass capillary. *h*. Device is loaded inside silicone tubes and filled with epoxy. *i*. Epoxy is cured. *j*. Extra epoxy is trimmed off and the device is ready for functional testing.

D1 and regulated by Zener diodes and filter capacitor C3 to provide a constant charging voltage Vs = +16 VDC. While the RF signal is being transmitted, capacitor Cout is slowly charged through a circuit consisting of limiting resistor R1 and the electrodes (modeled as a series Ctissue and Rtissue in Fig. 3). As long as the voltage on Cout is below Vs, the PUT remains in a high impedance state. When the RF signal is removed, Vs drops quickly to zero and the PUT goes into a low impedance state that rapidly discharges Cout through the electrodes, creating the effective stimulation pulse. For each stimulus output pulse, the amount of charge that the output capacitor delivers is precisely controlled by the duration of the transmitted RF burst, which ranges from 120μs to 19.9ms. A set of 20 burst durations generate a set of pulse strengths that form an exponential series from approximately 0.05 to 4.9 μC in which each successive step represents about 27% increase over the previous step. The repetition rate can be controlled from 1 to 50 pulses per second (pps). The output is charge-balanced, capacitively-coupled with a cathodal stimulus phase that has a time-constant of approximately 0.33 ms duration

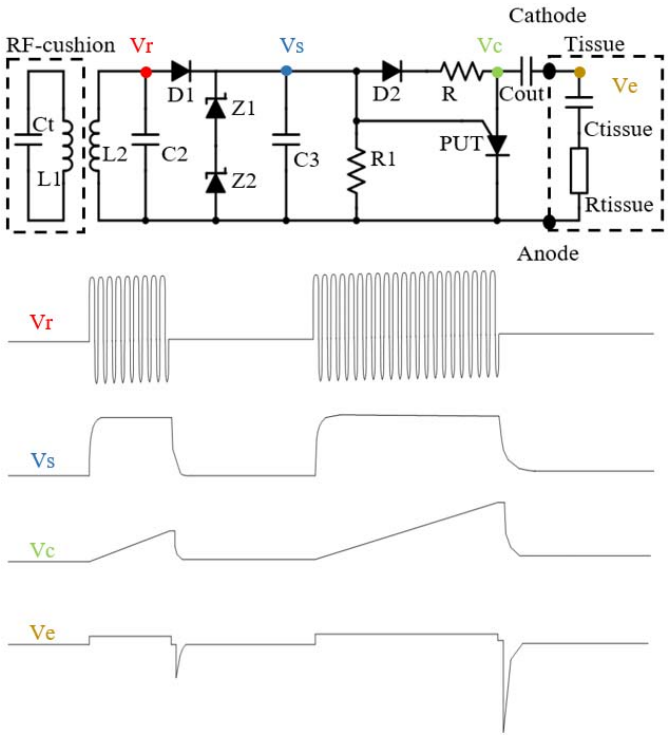

Fig. 3. Schematic circuit and conceptual waveforms of the NuStim implant for two output pulses with low and high charge, respectively. L2 = 11.5μH. C2 = 47pF. C3 = 3.3nF. R1 = 1MΩ. R = 39kΩ. Cout = 0.33μF.

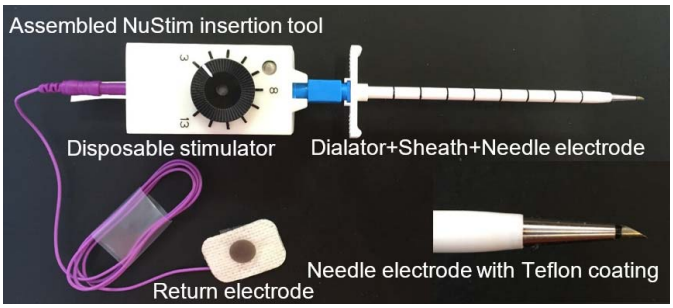

Fig. 4. Assembled NuStim insertion tool. The dilator (3.26 mm o.d. × 117.6 mm length) passes through the sheath (4.27 mm o.d.).

when the tissue impedance is approximately 1 kOhm. For comparison, a square pulse with 10 mA amplitude and 0.33 ms duration represents 3.3 μC, similar to the maximal output of the NuStim.

C. Insertion Tool

The implantation and deployment strategy utilizes a sterile NuStim insertion tool consisting of a needle electrode inside a dilator inside a sheath plus a disposable handheld stimulator (Fig. 4). The NuStim implantation can be performed as an outpatient procedure under local anesthesia in a lithotomy position. A low threshold implantation site is first located using a disposable hypodermic EMG needle (Fig. 5a) connected to the handheld stimulator via a pinjack adapter. The return electrode is connected to the back of the handheld stimulator and attached to the skin. A skin incision is made at a different location as an entry site for the NuStim insertion tool to be oriented approximately perpendicular to the perineum, and

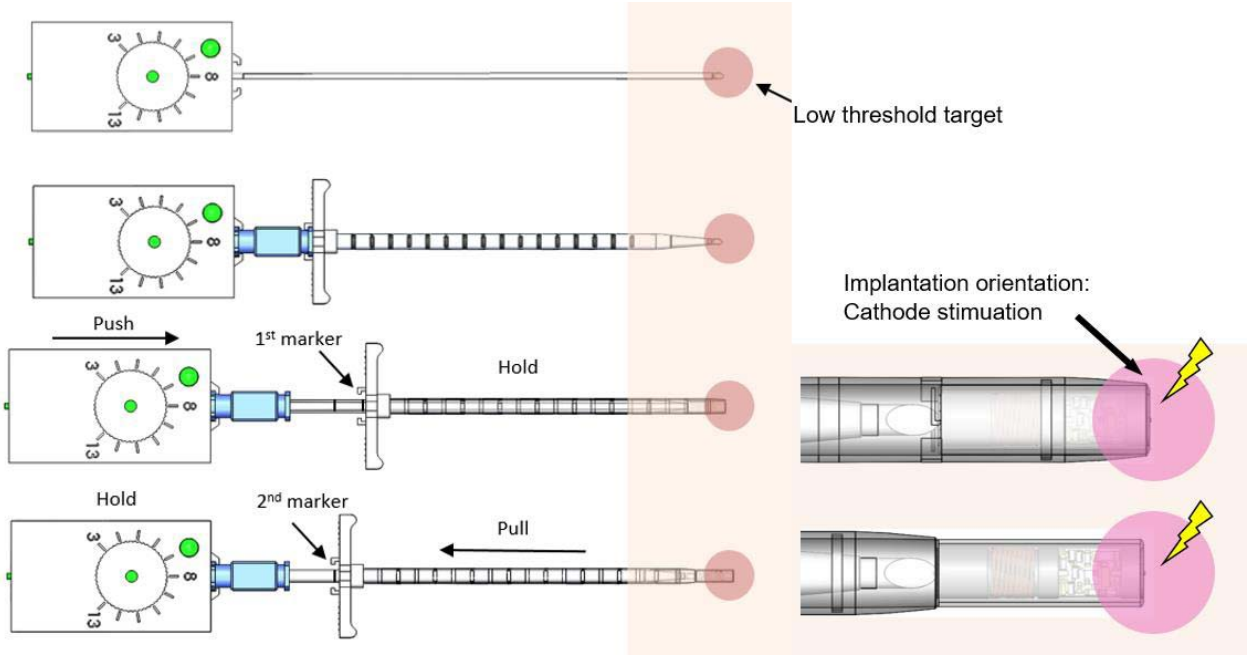

Fig. 5. *a*. A Teflon-coated needle electrode with sharp beveled tip is connected to the disposable stimulator. The needle is used to find the low-threshold target stimulation site. *b*. The assembled insertion tool is used to locate the low-threshold target identified with the needle. *c*. Stimulation charge is passed through NuStim to confirm the low-threshold target site. *d*. The NuStim is released at the targeted stimulation site.

aimed so that the end of the needle is at approximately the target determined above. The insertion tool with its needle electrode attached to the handheld stimulator is advanced in 1 cm steps toward the target while applying stimulation pulses that are calibrated to the same clinical units as produced by the NuStim implant (Fig, 5b). The threshold for a visible twitch decreases as the needle electrode approaches the motor axons, then increases after passing them in the next step. The stimulator with needle electrode and dilator are removed without moving the sheath, leaving the end of the sheath at the location where the threshold minimum was obtained. The NuStim is placed into the sheath with cathode facing the tissue. The needle + dilator is used to push the NuStim through the sheath to its tapered end, where there is a snug fit and some resistance (Fig. 5c). When the needle on the stimulator makes contact with the back of the NuStim implant, the stimulation pulses pass through the implant to its cathodal stimulating electrode, which is used to confirm the lowest threshold that was obtained previously. The NuStim is finally released to its site as the sheath is retracted over the dilator (Fig. 5d).

D. Cushion

1) Electrical: The sequence of stimulus pulses for each exercise cycle are sent to the microcontroller unit (MCU) in the external RF-Cushion from the Android tablet via BLE communication, which then generates a sequence of RF bursts with the required durations and intervals. The RF driver is operated at 6.78 MHz, an ISM (Industrial-Scientific-Medical) band exempt from FCC limits on emitted field strength. This RF carrier signal is modulated and amplified at the buffer circuit to drive Q1 (IRLR024 N-channel MOSFET, VISHAY, CA), which is operated in a high power and highly efficient Class-E configuration to feed the antenna (Fig. 6). The ideal calculation and practical tuning procedure of the class E amplifier is based on Sokal's method to keep voltage and current out of phase by means of a stagger-tuned LC circuit [16]. The output impedance of the class E amplifier and the input impedance of the primary coil loaded by the dissipative tissues of the body are matched to 50-ohms impedance for efficient power transmission. The MOSFET achieves desired 50% duty cycle and draws 18W from +12 VDC supply. The voltage driving the 50Ω impedance is 40V which represents about 89% power efficiency. The electromagnetic field strength of the RF-Cushion was calculated theoretically and measured by a calibrated detection coil (2 turns on 17.5 mm radius, 18AWG insulated copper wire) [15] with the body load simulated as a saline solution inside a toroidal inner tube (Figs. 7a and b).

The physical size of the primary coil is confined by the 24 cm diameter of the seat cushion. Two turns of wide copper trace create 15 A/m field strength up to 10 cm distance from the plane of the coil, the maximal anticipated depth of the NuStim in patients. The minimal field strength required to reach Zener-regulated voltage in the implant is approximately 10 A/m. The primary coil is optimized to have 50Ω input impedance when the subject is actually present, which allows maximal output efficiency. The mismatch that occurs when the patient is not present is detected by the load detection circuit, which then turns off the exercise session. Current and temperature detection are used to prevent circuit damage from excessive loading such as might occur if the cushion is placed on a conductive metal surface.

2) Mechanical: The primary coil and external electronics are populated on a 4-layer PCB board that is embedded in the RF-Cushion. The electronic circuit has an aluminum cover on top and bottom for heat dissipation and electromagnetic

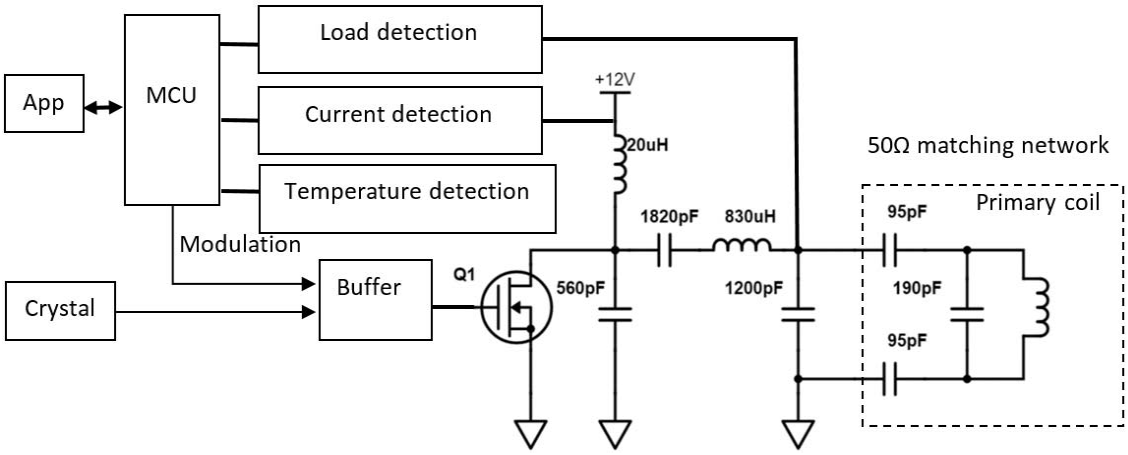

Fig. 6. RF-Cushion system architecture.

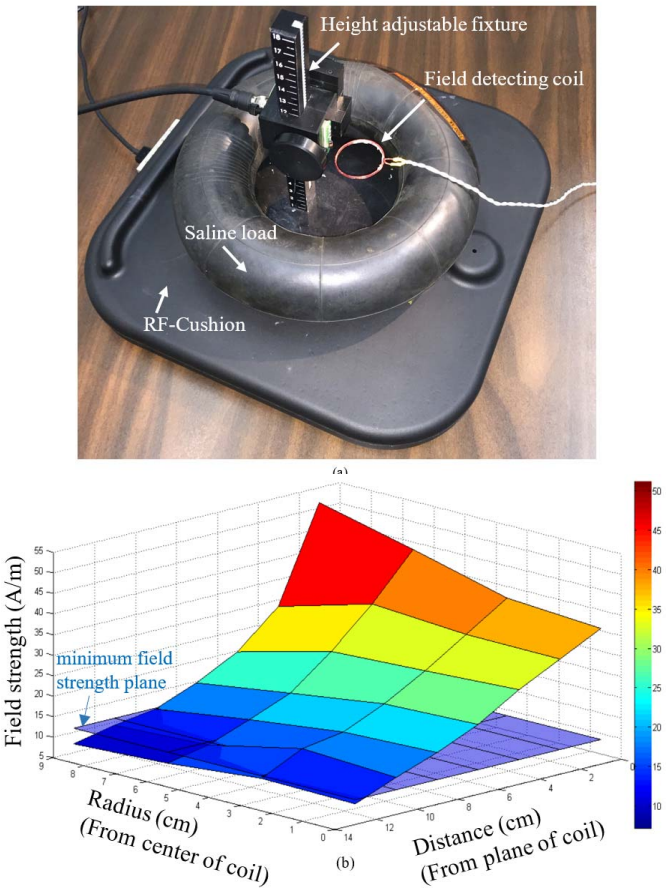

Fig. 7. *a*. NuStim system test configuration with saline tube to simulate dissipative loading by conductive tissues of the body. *b*. The electromagnetic field strength measured from the center to the edge of the primary coil (radius) as the distance is increased. The blue plane indicates the minimum field strength needed for regulated stimulation. The intersection with the measured field strength indicates the maximum operating range of the device.

shielding. The RF-Cushion has an outer shell of waterproof polyurethane foam with no exposed electrical components or controls, and thus should avoid an electrical shock hazard even if the patient leaks urine. The electronic components face the bottom of the RF-Cushion to decrease the foam thickness between the subject and primary coil. The exposed end of the aluminum cover has a LED power indicator and a magnetic power port for connection to a medical-grade 12 VDC power supply.

E. Software App

The software application has two functions: to allow a physician to identify the appropriate range of stimulus strength and exercise program for a given patient, and to allow the patient to adjust stimulation within that range to obtain and track the prescribed exercise.

In physician mode, the system provides a range of 20 stimulus intensities that can be adjusted from threshold to target level while generating single twitches at 2 pps stimulation frequency. The threshold level is based on identification of first twitch sensation at the lowest stimulus; the target level is identified as maximal strength twitch or maximal comfortable level, whichever comes first. After these intensities are locked, stimulation cycle parameters are then selected to provide strong, cyclical contractions and relaxations for the desired exercise period (typically 30-60 minutes/day). During each exercise cycle at the selected repetition rate, the pulse intensity ramps up from threshold to the selected intensity level, holds at that level, and then ramps down, followed by a pause between cycles (Fig. 8a). After the clinician tests these exercise cycles (screenshot in Fig. 8b), the subject can take home their RF-Cushion paired with a tablet computer on which the prescribed exercise parameters have been stored.

In patient mode, the subject is instructed to self-administer the prescribed exercise on a daily basis. The subject can only adjust the stimulus intensities over the range from the determined threshold to target in a scale that goes from 1-10 in linear steps of RF burst duration (Fig. 8c). The prescription allows the patient to go beyond that range up to 150% by linear extrapolation (limited to the maximal RF burst duration of 20ms). The app is designed to encourage the patient to use the highest comfortable stimulus strength from the range prescribed by the physician, which can result in accomplishing the prescribed daily exercise in the shortest period of time according to an algorithm for tracking adherence to treatment

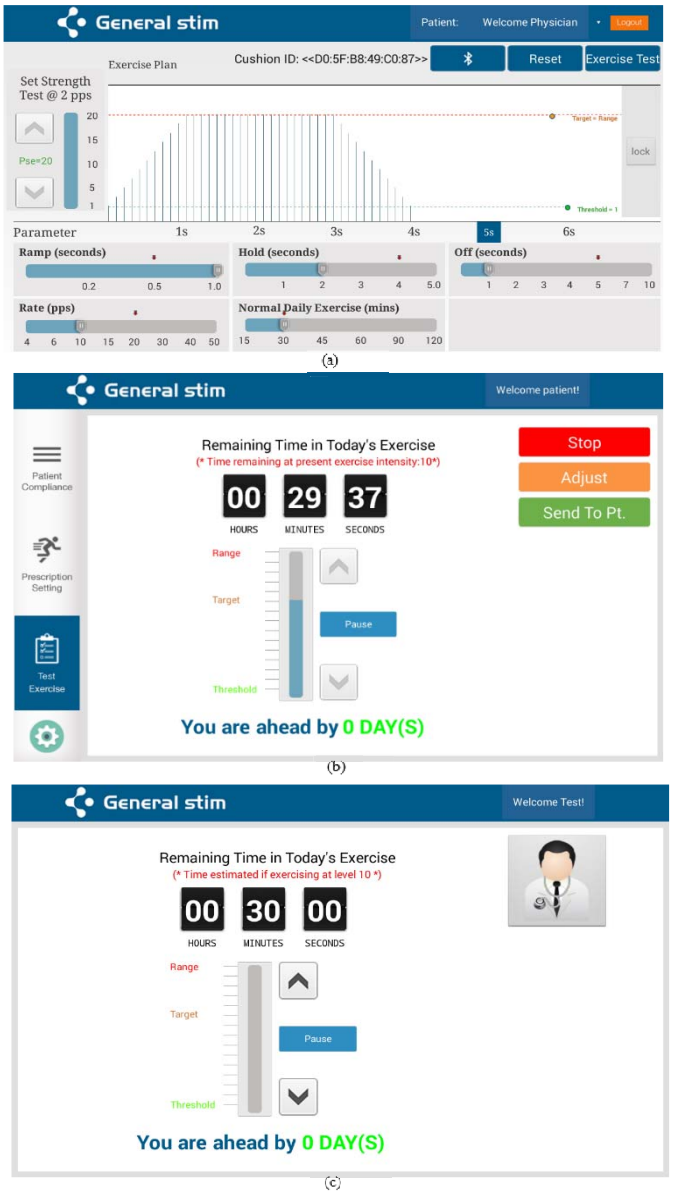

Fig. 8. *a*. Prescription mode. Various stimulation parameters are determined by the physician on tablet. *b*. Prescription testing mode. Exercise is first tested in the prescription testing mode before being sent to the patient. *c*. Patient mode. Patient performs the prescribed exercise at home.

in the tablet. The app keeps track of whether the patient is ahead or behind the prescribed daily regimen. All adherence information can be read out by during follow-up visits.

III. Methods

A. Verification In Vitro

Tests were performed *in vitro* to verify the functionality of the NuStim system. A saline-filled inner tube was placed on the RF-Cushion to simulate human tissue load (Fig. 7a). The microstimulator was placed in a fixture with spring-loaded probes to connect the electrodes to a 1 kOhm resistive load. The stimulus intensity was adjusted on the software APP from level 1 to level 20 while the implant was positioned at different heights and angles from the RF-Cushion. Various exercise patterns (different stimulation parameters: ramp, hold, off, pps and exercise time) were adjusted on the software APP to validate the complete system. Stimulus output from the microstimulator was measured on an oscilloscope screen to verify that the stimulus generation meets requirements for sufficient muscle activation.

B. Preclinical Validation In Vivo

Before the NuStim system can be used clinically, chronic animal experiments are needed to provide evidence of safety and efficacy. The objectives of the animal study were i) to identify the feasibility of the minimally invasive implantation procedure, ii) evaluate the complete system for threshold level identification and muscle activation on a daily basis, and iii) to evaluate the short and long term device stability and tissue response via threshold measurement and histology. The animal experiments conformed to the Guide for the Care and Use of Laboratory Animals and were approved by the Institutional Animal Care and Use Committees at the Capital Medical University, Beijing, China. Experiments were carried out on three adult beagle dogs (9.4 to 11.2 kg) sedated with 2 to 3 ml Xylazine and anesthetized with sodium pentobarbital (2.5%, 1 ml/kg intramuscular). NuStim implants and insertion tools were sterilized in ethylene oxide and implanted using aseptic technique. A total of five active devices were implanted into quadriceps femoris or triceps brachii and exercised daily for two weeks. Four non-activated devices were placed in the comparable contralateral muscles. Insertions were directed perpendicularly to the skin in order to orient the devices transversely to the muscle fibers, but there was no attempt to correct for the substantial pennation angle of these muscles. The insertion tool was used to locate the depth at which the threshold to evoke a muscle twitch was minimal; once identified, the NuStim was deposited at this site. Non-active devices were implanted without regard to optimal stimulation site. The animals recovered for at least 7 days after implantation before initial activation. The threshold was measured for each active device at least once per week. Daily exercise was performed in the first two weeks for each active implant at an intensity that produced an apparently maximal twitch, using pulse trains intended for clinical use (0.5s ramp, 4s holding, 5s off, 6 pps and 30 min/day exercise period). The prescribed exercise pattern was designed empirically to simulate the voluntary PFMT with a cyclical, voluntary squeeze and relaxation of the muscle for a few seconds with repetition up to 1 hour a day [3]. The stimulus pulse rate was limited to 6 pps to avoid hyperextension from tetanic contraction.

At the end of study, Dog 1 had been implanted for 98 days, Dog 2 for 27 days and Dog 3 for 72 days. All three were euthanized with intravenous potassium chloride and the implant sites were examined for gross and histological pathology. Tissue was fixed in 10% formalin for 7 to 10 days before removing the device and blocking for paraffin embedding and sectioning. Sections were obtained from tissue near the middle of the cylindrical device (3.4 mm diameter x 10.0 mm long) and were oriented perpendicularly to its long axis. The tissue was stained with hematoxylin and eosin (H&E) and examined under a light microscope.

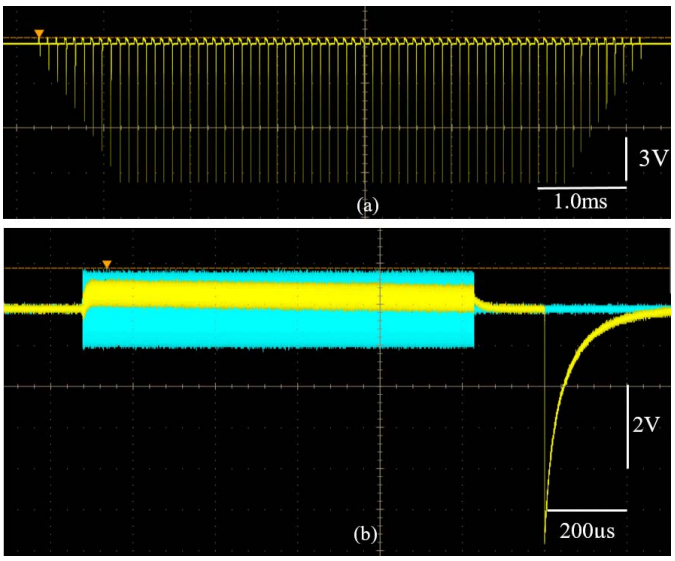

Fig. 9. *a*. Train of stimulation pulses delivered from the NuStim implant. (parameter settings: Threshold = 1, Target = 20, ramp = 1s, hold = 2s, off = 1s, frequency = 10 pps). *b*. NuStim output as measured on oscilloscope for stimulus level = 13 (yellow trace). Electromagnetic field generated from RF-Cushion in cycle of charging period (blue trace).

IV. Results

A. System Bench Testing

Trains of stimulus pulses prescribed by the software were generated as illustrated in Fig. 9a. The peak cathodal voltage of each stimulus pulse (yellow trace in Fig. 9b) was compared to the theoretical value expected according to the charge accumulated on Cout by the regulated Vs flowing through limiting resistor R for the period of time during which the RF carrier was on (blue trace in Fig. 9b). Fig. 10a plots the output voltages (log scale) obtained for each of the 20 clinical steps when the device was placed at various distances above the center of the RF cushion. For distances up to 10.5 cm and tilt angles to 45° from vertical as shown in Fig. 10b, the values agree closely with the theoretical value. This indicates sufficient power was received to activate the Zener diodes that clamp Vs at +16 VDC. The dotted red trace indicates how the output would have decreased according to the cosine of the tilt angle without the presence of the ferrite core. The stimulus output charge (orange trace in Fig. 10c) was compared to the theoretical value (blue trace in Fig. 10c) of the 20 clinical steps. Each marker represents a clinical step in the app. The measured stimulus charge follows the same exponential curve as the ideal calculation, but an increasing difference from the ideal calculation was observed for the six highest stimulus charge values.

B. System Validation In Vivo

When properly positioned over the RF-Cushion, each active implanted devices was activated separately to cause muscle contractions that could be palpated on the skin and observed as cyclical limb motion. When the repetition rate was above 20 pps, the muscle contraction was smooth and sufficient to fully extend the limb. The animals generally ignored the stimulation in the course of exercise without sedation, but required custody and petting to stay on the RF-cushion during

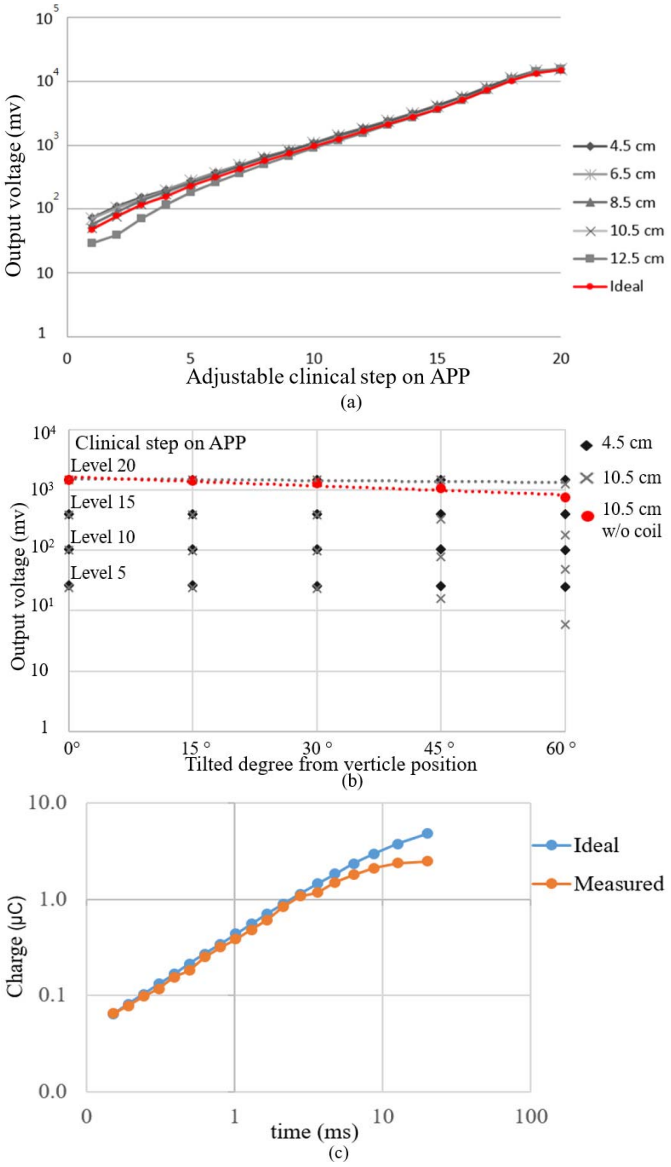

Fig. 10. *a*. NuStim output measured at different distances from the plane of primary coil as a function of stimulus strength steps in the app. b. NuStim output measured at different tilted angle, height and intensity level. Dotted red trace is calculated output decreased as the tilted angle without presence of ferrite at level 20. *c*. Stimulus charge comparison between measured values and ideal calculation at the RF burst durations programmed to produce the 20 stimulus step values.

the exercise. Sedation was administered for most of the daily 30-minute exercise periods for convenience. Thresholds for implanted devices were all in the range of 6 to 9 clinical units when initially activated 10 days after implantation. Fig. 10a shows trends in the thresholds over time normalized to the value on the activation day and compared to the thresholds obtained during implantation on day zero. The target stimulus strength needed to generate apparent maximal twitch was different for each device. The active device in Dog 1 vastus muscle only required 3 to 4 clinical units above threshold while the device in Dog 2 produced more gradual increases in recruitment over 11 steps. One of the 5 active devices ceased to produce stimulation pulses 5 days after implantation. Electrical function testing of this device removed at necropsy showed

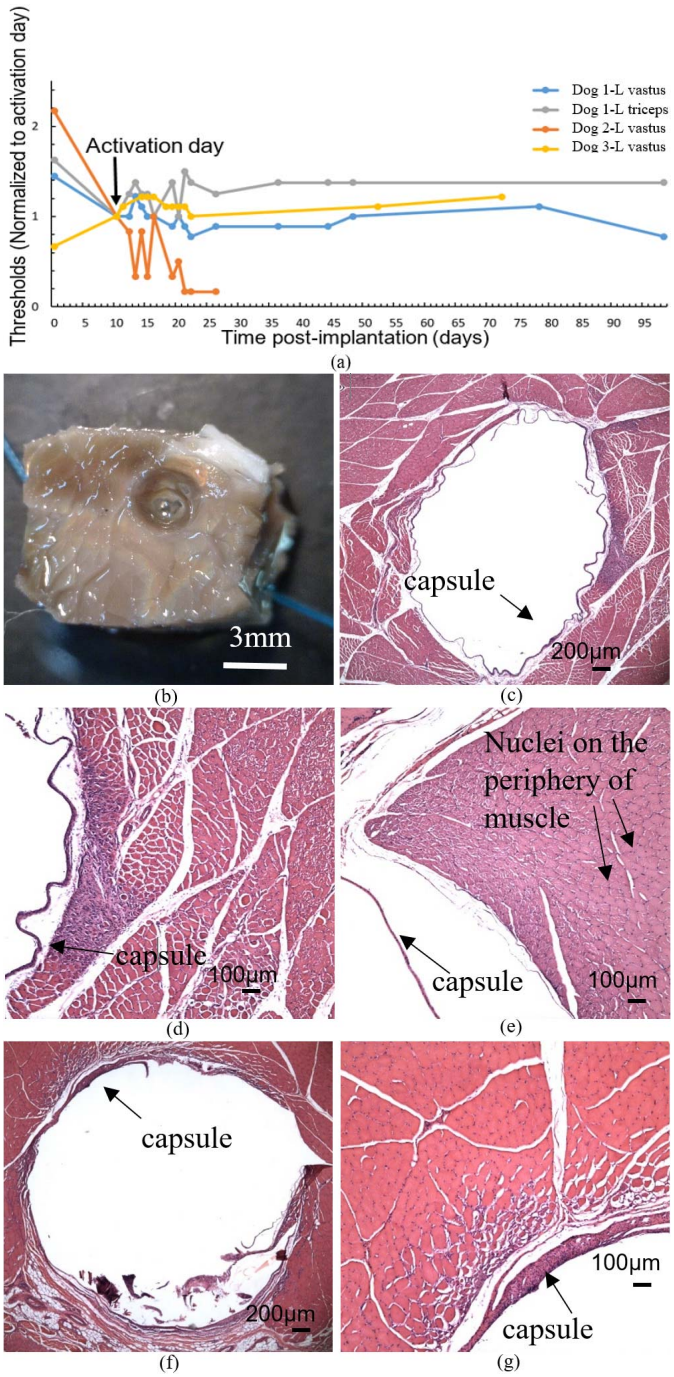

Fig. 11. *a*. Threshold measurements as a function of post-implantation day (normalized to implant activation day). *b*. Muscle block with a capsule after active device removal. *c*-*e*. Photomicrographs of a tissue section stained with H&E from the block in *d* showing typical features of cellular response and capsule formation 1 month after implantation. *e*. Typical histological appearance around active device after 3 months. *Zf and g*. tissue section from control side with typical appearance around non-active device after 3 months.

that it no longer resonated at the tuned frequency. The most likely cause would be a cold solder joint where the copper wire is attached to the ceramic PCB. This failure mode was subsequently mitigated with a manufacturing change to pretin the copper wire before soldering to the PCB.

Each implanted muscle was removed at necropsy with the device left in the tissue block. All active and passive devices were well-integrated with surrounding tissues, which made them somewhat difficult to find. There were no gross pathological signs of reaction or infection. Tissues from which active and non-active devices were removed after fixation are shown in Figs. 11b to g. The capsule layer was peeled away from the surrounding tissue in some places, presumably because of forces on the tissues during device extraction, but remained in position in most samples. The thickness of the fibrotic capsule around the three month implants (Fig 11.e) was about half as thick as that after one month (Fig 11.d). Close to the capsule, there were some small muscle fibers with central nuclei suggestive of ongoing recovery from damage during the initial implantation. Further from the capsule, the myonuclei were spaced around the periphery of the muscle fibers in a normal pattern for healthy muscle fibers. Around the longer term implants, the unaffected muscle fibers were closer to the capsule, which suggests progressive healing of local insertion trauma. Muscle fibers immediately adjacent to the capsule tended to be cut transversely (i.e., running parallel to the long axis of the cylindrical implant) but further away the plane of section appeared to be more oblique, consistent with the intent to implant the device transversely to the muscle fibers. The mechanical presence of the device may have resulted in some local reorientation of muscle fibers, particularly those recovering from implantation damage. Some of the non-active devices were found wholly or partially in loose connective tissue rather than within a muscle (Fig 11.f). Their surrounding capsules tended to collapse from lack of support by fixed muscle when the implants were removed prior to embedding and sectioning. No clinically significant histological differences were observed between the active and passive devices at the same time points.

V. Discussion

The NuStim system described here successfully meets the design requirements. We validated that the Android software app allowed researchers to adjust stimulation parameters to accommodate substantial differences in orientation of the implant with respect to the local motor axons that are the target of the neuromuscular stimulation. The RF-Cushion responded to these commands and generated a sufficiently strong magnetic field to allow the implant to generate the requested stimulus charges over the desired range of distances and orientations.

Some of the voltage and charge measurements *in vitro* were lower than calculations predicted. The output voltage for the lowest charge pulses decreased slightly as the distance increased between the secondary and primary coil. Generally, the RF-Cushion requires about 30 cycles for the class E amplifier to ring up to full field strength. When the implant is further from the transmitter, it reaches the regulated voltage later in this ramp. For the lowest charge pulses, this delay becomes a noticeable portion of the relatively brief RF burst. Such variability might be a concern for other applications requiring accurate control of partially recruited muscles, but it is not critical for the proposed SUI application, which aims for strong stimulation to achieve complete muscle recruitment. The difference between the measured and calculated

charge for the highest clinical steps is mostly due to the nonlinearity of the multilayer ceramic output capacitor Cout (C1005X5R1E334K050BB, TDK Corporation). This is the only commercially available capacitor with a combination of acceptable capacitance, voltage rating and small package size for the application. The capacitance of C2 decreases nonlinearly as the bias voltage across the capacitor increases, making the capacitor is less able to store charge at the higher voltages associated with the highest clinical levels. The physiological efficacy of these pulses is actually less affected than the reduction in delivered charge because the missing charge would have been delivered in the exponential tail of the stimulus pulse, which is well after the 150μs time constant of the myelinated motor axons.

The animal study confirmed that the insertion tool could be used to implant the device in a low-threshold location where strong skeletal muscle contraction could be achieved ($<$ clinical step level 13 $=\sim$0.8 μC) well before reaching the maximal measured output of the NuStim implant (about 3 μC). A significant change of threshold after implantation may indicate migration through or damage to surrounding tissue. Proper healing after implantation is necessary for implant stabilization. The stability of the threshold values over an extended period of electrically induced muscle contractions suggests that the implants did not migrate or damage the muscle. The connective tissue capsule that starts to form around cylindrical implants in the first few days after implantation [17] gradually becomes less reactive and better integrated into the endomysial connective tissue that surrounds and supports all muscle fibers [18]. The absolute value of the threshold was expected to differ between implantations because it is quite sensitive to the distance between the cathodal electrode and the nearest motor axons. Accordingly, the rate at which twitch force increases with stimulus strength depends on the distribution of intramuscular nerve branches with respect to the implant, which is likely to vary considerably depending on the neuromuscular architecture of the muscle and the location of the stimulator [19]–[21]. Healing and local reorganization of tissues after implantation (as well as uncertainties in palpating twitch threshold in an awake animal) are the likely cause of the small shifts in electrical thresholds noted after implantation. Similar encapsulation and recruitment patterns were described previously for BION stimulators [22]. The physician can palpate contractions of the pelvic floor muscles, but we expect that it will be simpler and perhaps more accurate to rely on the patient's perception of the electrically induced muscles contractions.

NuStim implants with non-hermetic epoxy packaging were found in most cases to maintain functionality for the limited duration of these experiments (about 3 months). The one failure appeared to be an idiosyncratic flaw during manufacturing rather than an encapsulation failure. Similar devices have been subjected to an accelerated life-test that involves soaking in saline at 50°C while operating at continuous maximal output (article in preparation). This methodology was used to refine the cleaning and encapsulation processes described in this article. The NuStim is made from inert, biocompatible materials that may be left in the body permanently, similar to medical devices such as nonresorbable sutures, vascular clips and orthopedic bone screws. If there is a medical indication for NuStim removal such as infection or pain, this will require a minor surgical procedure under local anesthesia, probably with ultrasound guidance to locate the implant easily.

There are no good animal models for SUI in humans. One animal model of urinary incontinence used surgical dissection of the muscle surrounding the urethra, which is likely to damage the muscle nerve in a manner that is unlike human SUI [23]. It is impractical to incorporate the extended periods of *post partem* reorganization and post-menopausal hormone withdrawal that characterize most clinical cases of SUI. Furthermore, terrestrial quadrupeds do not require pelvic floor muscles as strong as a human, which must support pelvic viscera during upright posture. The canine quadriceps and triceps have sufficient thickness for transverse implantation, similar to the implantation orientation expected in the human pelvic floor, and they facilitate visual monitoring of muscle recruitment. The chronic animal experiment presented here confirms that the NuStim can produce strong, well-controlled, repetitive contractions in skeletal muscle. It remains to be demonstrated that exercise patterns similar to PFMT can be obtained in the skeletal muscle of the human pelvic floor, which has similar neuromuscular physiology and size but somewhat different innervation and fiber architecture.

The RF magnetic field strength required to achieve inductive power transmission over the required distance must be considered in terms of the specific absorption rate (SAR) allowed by the guidelines/standards [24]. Tests of a similar wireless transmission system for a fetal micropacemaker indicated that about 50% of the applied magnetic field was absorbed by eddy currents induced in the conductive tissues of the body [15]. This corresponds to about 8 Watts of energy from the NuStim RF-Cushion (peak value when the RF burst is on), which will be dissipated as heat in the pelvic region overlying the transmission coil. If we model that region as a cylinder with 0.1 m radius and 0.1 m height and specific gravity of 1.0, we get a 3.1 kg mass. The foam insulation layer of the RF-Cushion ensures that no tissue will be in direct contact with transmission coil. The app software was programmed to limit the RF duty cycle to avoid overheating the circuitry in the RF-Cushion. For example, when the stimulus intensity is maximal at level 20, the clinician cannot prescribe a stimulation frequency greater than 20 pps, which produces a strong, smooth contraction in skeletal muscle. After allowing for the minimal off-time between stimulus trains, the maximal RF duty cycle is 35%. This corresponds to 0.9 W/kg, well below the 1.6 W/kg safety limit.

Eddy currents induced by very strong magnetic fields have been used to excite pelvic nerves and muscles for exercise therapy of SUI. It avoids the need for vaginal or anal electrodes but it is poorly selective, leading to unwanted sensory and motor effects, even when the patient is positioned optimally and the magnetic field strength is adjusted carefully by a clinician [25]. The NuStim must be implanted in a simple outpatient procedure, but it then appears likely to enable selective and consistent recruitment of just the target muscle when used by the patient at home. It remains to be determined whether

some patients will require implants in both sides of the pelvic floor.

The NuStim provides a wide range of stimulation parameters with which to treat SUI. It remains to be determined which stimulation patterns will be both comfortable for the patients and effective and efficient to exercise the EUS muscle to treat SUI. For typical SUI patients with severe EUS atrophy, muscle fibers are easy to fatigue. Slow-twitch muscle fibers are non-fatiguing, and thus are capable of continuous or frequent contractions for urethral closure at rest. Fast-twitch muscle fibers are more easily fatigued but can respond more rapidly and forcefully to sudden recruitment (e.g., during coughing). Low-frequency and high-intensity electrical stimulation tends to reverse disuse muscle atrophy, building bulk and peak force generation [26]. Longer cycles of stimulation with intermediate frequencies and longer exercise periods tend to improve fatigue resistance [27]. High frequency bursts of stimulation produce maximal contractile force. It is unclear how patients may tolerate the sensations produced by these different patterns of muscle contraction. The pulse train used in the animal study is the default exercise pattern for clinical use. The planned pilot clinical study is intended to identify stimulus and exercise parameters that achieve a useful balance of acceptability for the subjects and clinical improvement of SUI. The usability of the clinical system and its software APP by physicians and patients will be tested in the clinical trial.

ACKNOWLEDGMENT

The authors would like to thank Xing Li, Tianji Lu, Zhaoxia Wang and Han Deng for assistance in animal care, Dr. Frances J. Richmond for assistance with histological analysis, consultant Thomas Yeh for software development and engineers Ray Peck, Gary Lin, Sisi Shi, and Longpeng Jiao for contributions to design and manufacture.

REFERENCES

[1] S. Hunskaar, E. P. Arnold, K. Burgio, A. C. Diokno, A. R. Herzog, and V. T. Mallett, "Epidemiology and natural history of urinary incontinence," *Int. Urogynecol. J.*, vol. 11, no. 5, pp. 301–319, Sep. 2000.

[2] A. Grimby, I. Milsom, U. Molander, I. Wiklund, and P. Ekelund, "The influence of urinary incontinence on the quality of life of elderly women," *Age Ageing*, vol. 22, no. 2, pp. 82–89, Mar. 1993.

[3] C. Dumoulin, E. J. C. Hay-Smith, and G. M. Habée-Séguin, "Pelvic floor muscle training versus no treatment, or inactive control treatments, for urinary incontinence in women," *Cochrane Database Syst. Rev.*, vol. 1, no. 1, pp. 1–54, May 2010.

[4] K. Bø, "Pelvic floor muscle training is effective in treatment of female stress urinary incontinence, but how does it work?" *Int. Urogynecol. J.*, vol. 15, no. 2, pp. 76–84, Mar./Apr. 2004.

[5] E. S. Rovner and A. J. Wein, "Treatment options for stress urinary incontinence," *Rev. Urol.*, vol. 6, no. Suppl 3, pp. 29–47, 2004.

[6] E. Petri and K. Ashok, "Comparison of late complications of retropubic and transobturator slings in stress urinary incontinence," *Int. Urogynecol. J.*, vol. 23, no. 3, pp. 321–325, Mar. 2012.

[7] D. Y. Deng, M. Rutman, S. Raz, and L. V. Rodriguez, "Presentation and management of major complications of midurethral slings: Are complications under-reported?" *Neurourol. Urodyn.*, vol. 26, no. 1, pp. 46–52, Jan. 2007.

[8] T. Yamanishi, T. Kamai, and K.-I. Yoshida, "Neuromodulation for the treatment of urinary incontinence," *Int. J. Urol.*, vol. 15, no. 8, pp. 665–672, Aug. 2008.

[9] K. Bø, T. Talseth, and I. Holme, "Single blind, randomised controlled trial of pelvic floor exercises, electrical stimulation, vaginal cones, and no treatment in management of genuine stress incontinence in women," *BMJ*, vol. 318, pp. 487–493, Feb. 1999.

[10] N. T. M. Galloway, R. E. S. El-Galley, P. K. Sand, R. A. Appell, H. W. Russell, and S. J. Carlan, "Extracorporeal magnetic innervation therapy for stress urinary incontinence," *Urology*, vol. 53, no. 6, pp. 1108–1111, Jun. 1999.

[11] K. P. Caldwell, "The treatment of incontinence by electronic implants. Hunterian lecture delivered at the Royal College of Surgeons of England on 8th December 1966," *Ann. Roy. College Surgeons England*, vol. 41, no. 6, p. 447, 1967.

[12] G. E. Loeb, R. A. Peck, W. H. Moore, and K. Hood, "BION system for distributed neural prosthetic interfaces," *Med. Eng. Phys.*, vol. 23, no. 1, pp. 9–18, Jan. 2001.

[13] G. E. Loeb, F. J. R. Richmond, and L. L. Baker, "The BION devices: Injectable interfaces with peripheral nerves and muscles," *Neurosurgical Focus*, vol. 20, no. 5, pp. 1–9, May 2006.

[14] P. E. K. Donaldson, "The essential role played by adhesion in the technology of neurological prostheses," *Int. J. Adhes. Adhesives*, vol. 16, no. 2, pp. 105–107, May 1996.

[15] A. N. Vest *et al.*, "Design and testing of a transcutaneous RF recharging system for a fetal micropacemaker," *IEEE Trans. Biomed. Circuits Syst.*, to be published.

[16] N. O. Sokal, "Class-E RF power amplifiers," *QEX Commun. Quart.*, vol. 204, pp. 9–20, Jan. 2001.

[17] T. L. Fitzpatrick, T. L. Liinamaa, I. E. Brown, T. Cameron, and F. J. Richmond, "A novel method to identify migration of small implantable devices," *J. Long-Term Effects Med. Implants*, vol. 6, nos. 3–4, pp. 157–168, 1997.

[18] J. A. Trotter, F. J. R. Richmond, and P. P. Purslow, "Functional morphology and motor control of series-fibered muscles," *Exerc. Sport Sci. Rev.*, vol. 23, no. 1, pp. 167–213, Jan. 1995.

[19] T. Cameron, F. J. R. Richmond, and G. E. Loeb, "Effects of regional stimulation using a miniature stimulator implanted in feline posterior biceps femoris," *IEEE Trans. Biomed. Eng.*, vol. 45, no. 8, pp. 1036–1043, Aug. 1998.

[20] H. Mino, J. T. Rubinstein, C. A. Miller, and P. J. Abbas, "Effects of electrode-to-fiber distance on temporal neural response with electrical stimulation," *IEEE Trans. Biomed. Eng.*, vol. 51, no. 1, pp. 13–20, Jan. 2004.

[21] R. B. Stein, D. J. Weber, K. M. Chan, G. E. Loeb, R. Rolf, and S. L. Chong, "Stimulation of peripheral nerves with a microstimulator: Experimental results and clinical application to correct foot drop," in *Proc. 9th Annu. Conf. Int. FES Soc.*, 2004, pp. 1–3.

[22] T. Cameron, T. L. Liinamaa, G. E. Loeb, and F. J. R. Richmond, "Long-term biocompatibility of a miniature stimulator implanted in feline hind limb muscles," *IEEE Trans. Biomed. Eng.*, vol. 45, no. 8, pp. 1024–1035, Aug. 1998.

[23] A. Hijaz, F. Daneshgari, K.-D. Sievert, and M. S. Damaser, "Animal models of female stress urinary incontinence," *J. Urol.*, vol. 179, no. 6, pp. 2103–2110, Jun. 2008.

[24] T. Shimamoto, M. Iwahashi, Y. Sugiyama, I. Laakso, A. Hirata, and T. Onishi, "SAR evaluation in models of an adult and a child for magnetic field from wireless power transfer systems at 6.78 MHz," *Biomed. Phys. Eng. Exp.*, vol. 2, no. 2, p. 027001, 2016.

[25] T. Yamanishi, Y. Homma, O. Nishizawa, K. Yasuda, and O. Yokoyama, "Multicenter, randomized, sham-controlled study on the efficacy of magnetic stimulation for women with urgency urinary incontinence," *Int. J. Urol.*, vol. 21, no. 4, pp. 395–400, Apr. 2014.

[26] A. C. D. Salter, F. J. R. Richmond, and G. E. Loeb, "Prevention of muscle disuse atrophy by low-frequency electrical stimulation in rats," *IEEE Trans. Neural Syst. Rehabil. Eng.*, vol. 11, no. 3, pp. 218–226, Sep. 2003.

[27] A.-C. D. Salter *et al.*, "First clinical experience with BION implants for therapeutic electrical stimulation," *Neuromodulation, Technol. Neural Interface*, vol. 7, no. 1, pp. 38–47, 2004.

Xuechen Huang received the B.S. degree in biomedical engineering (BME) from Southern Medical University, China, in 2012, and the M.S. degree in BME from the University of Southern California (USC), Los Angeles, CA, in 2014, where he is currently pursuing the Ph.D. degree in BME with the Viterbi School of Engineering.

Kaihui Zheng received the M.S. degree in biomedical engineering with the University of Southern California, Los Angeles, CA, in 2011. She was an Electrical Engineer with General Stim Inc. She is currently an Electrical Engineer with St. Jude Medical.

Sam Kohan received the B.S. degree in computer systems engineering from Western Michigan University, Kalamazoo, Michigan, in 1983.

He has various experiences in medical industry, including design of infusion pump and pulse oximeters. He is currently a Senior Electrical Engineer with General Stim Inc.

Petcharat May Denprasert received the B.S. degree in mechanical engineering from California State University, Los Angeles, CA, in 2016. She was a Research Assistant with the University of Southern California in 2011. She is currently a Mechanical Engineer with General Stim Inc.

Limin Liao is currently a Professor of Urology with Capital Medical University (CMU), Beijing, China. He is also the Chairman of the Department of Urology, China Rehabilitation Research Center, Beijing, and the Director of the Ph.D. Training Program on Neurourology and Urodynamics with the Rehabilitation School, CMU.

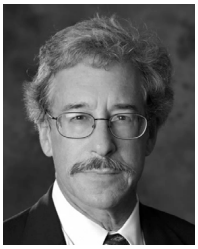

Gerald Eli Loeb (M'80) was with NIH, Johns Hopkins University, from 1973 to 1988, and a Professor in physiology with Queen's University from 1988 to 1999. He is currently a Professor of Biomedical Engineering and the Director of the Medical Device Development Facility, University of Southern California, Los Angeles, CA.